

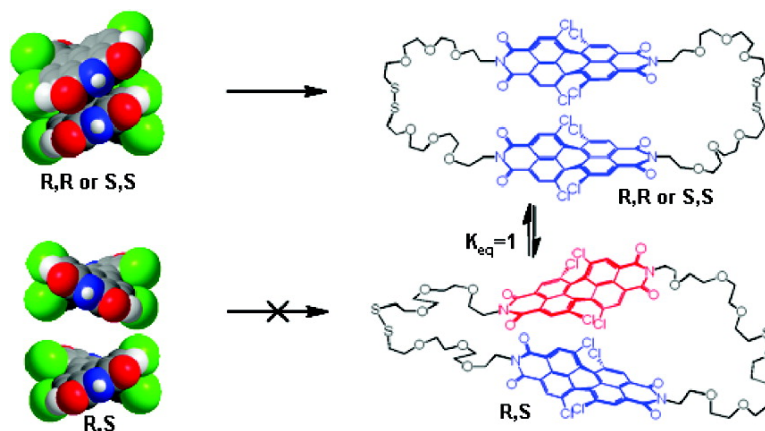
Article

## Twisted Perylene Stereodimers Reveal Chiral Molecular Assembly Codes

Wei Wang, Andrew D. Shaller, and Alexander D. Q. Li

*J. Am. Chem. Soc.*, **2008**, 130 (26), 8271-8279 • DOI: 10.1021/ja7111959 • Publication Date (Web): 10 June 2008

Downloaded from <http://pubs.acs.org> on February 8, 2009



### More About This Article

Additional resources and features associated with this article are available within the HTML version:

- Supporting Information
- Links to the 2 articles that cite this article, as of the time of this article download
- Access to high resolution figures
- Links to articles and content related to this article
- Copyright permission to reproduce figures and/or text from this article

[View the Full Text HTML](#)

## Twisted Perylene Stereodimers Reveal Chiral Molecular Assembly Codes

Wei Wang, Andrew D. Shaller, and Alexander D. Q. Li\*

Department of Chemistry, Washington State University, Pullman, Washington 99164

Received December 20, 2007; E-mail: dequan@wsu.edu

**Abstract:** Unique perylene diastereomeric linear and cyclic dimers were synthesized from twisted perylene monomers, revealing that  $\pi$ -stacking stereoisomerism imparted specific intermolecular self-assembly and intramolecular folding. Only the homochiral twisted tetrachloroperylene monomers cyclized via a cooperative reaction, forming the homochiral diastereomers. The heterochiral tetrachloroperylene monomers proceeded through a stepwise reaction and yielded a linear heterochiral dimer, which equilibrated with the linear homochiral dimers. The linear homochiral dimers cyclized to produce the same cyclic homochiral diastereomers. These results demonstrated that homochiral and heterochiral self-assemblies were two distinct molecular codes, directing two specific chemical pathways. The homochiral cyclic dimers remain isomerically pure at  $-20\text{ }^\circ\text{C}$  but can be interconverted to the heterochiral cyclic dimer meso compound at room temperature. The diastereomers were readily separated by HPLC. While driven by solvophobic forces, foldable linear dimers synthesized from the same twisted monomers using phosphoramidite chemistry folded into homodimer and heterodimer, confirming the inherent molecular codes, which were dictated by the perylene chirality, ultimately gauged the weak  $\pi$ -stack forces, and directed self-assembly and folding.

### Introduction

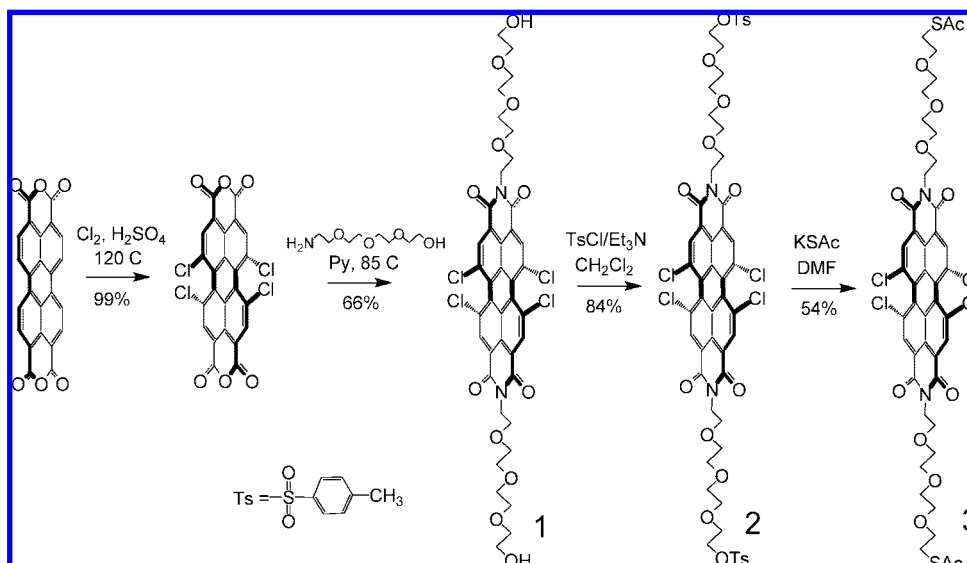
While covalent bonds establish the primary molecular structures, weak intra- and intermolecular forces govern molecular recognition and determine the folded or self-assembled supramolecular architecture. When the delicate balance of weak forces is reached, molecular assemblies such as DNA duplex and globular proteins establish their structure, gaining exquisite functionality. These weak forces typically include dispersion forces, hydrogen bonding, solvophobic effects, and Coulombic interactions.<sup>1</sup> Recently, however, more and more reports are focusing on the often overlooked weak  $\pi$ - $\pi$  stacking force, resulting from the molecular overlap of  $\pi$ -orbitals between planar aromatic systems.<sup>2</sup>

Molecular assemblies allow the capacity to mimic nature by directing specific reaction pathways that are otherwise difficult to achieve. Such assemblies have been successfully demonstrated to form cyclic and/or concatenated rings.<sup>3</sup> A popular

approach utilizes molecular templates to modulate the effective molarity of reactive groups, providing a bias for certain pathways over competing ones by increasing the proximity between reaction centers.<sup>4,5</sup> However, with molecular self-assemblies, no template is needed, as the reactants undergo the assembly process by self-templating.<sup>6</sup>

In our recent reports, the role of the  $\pi$ - $\pi$  stacking force driving dynamic intermolecular self-assembly and intramolecular folding has been elucidated with a series of architecturally diverse nanostructured foldamers (folded polymers) using planar perylenetetracarboxylic diimides (PDIs) as the building block.<sup>6,7</sup> We first demonstrated that the planar monomers with minimally steric but highly solubilizing flexible tetraethylene glycol (TEG) side chains will spontaneously self-assemble above a critical self-assembly concentration, even in the absence of solvophobic

- (1) (a) Whitesides, G.; Boncheva, M. *Proc. Natl. Acad. Sci. U.S.A.* **2002**, *99*, 4769–4774. (b) Li, S.; Yan, H.-J.; Wan, L.-J.; Yang, H.-B.; Northrop, B.; Stang, P. J. *J. Am. Chem. Soc.* **2007**, *129*, 9268–9269. (c) Wang, Z.; Medforth, C.; Shelnutt, J. *J. Am. Chem. Soc.* **2004**, *126*, 15954–15955.
- (2) (a) Hoeben, F.; Jonkheijm, P.; Meijer, E.; Schenning, A. *Chem. Rev.* **2005**, *105*, 1491–1546. (b) Saiki, Y.; Sugiura, H.; Nakamura, K.; Yamaguchi, M.; Hoshi, T.; Anzai, J. *J. Am. Chem. Soc.* **2003**, *125*, 9268–9269. (c) Meyer, E.; Castellano, R.; Diederich, F. *Angew. Chem., Int. Ed.* **2003**, *42*, 1210–50. (d) Busch, D. H. *Top. Curr. Chem.* **2005**, *249*, 1–65. (e) Gabriel, G. J.; Sorey, S.; Iverson, B. L. *J. Am. Chem. Soc.* **2005**, *127*, 2637–2640.
- (3) (a) Kieran, A. L.; Pascu, S. I.; Jarroson, T.; Gunter, M. J.; Sanders, J. K. M. *Chem. Commun.* **2005**, 1842, 1844. (b) Stoddart, J. F.; Tseng, H.-R. *Proc. Natl. Acad. Sci. U.S.A.* **2002**, *99*, 4797–4800. (c) Raehm, L.; Kern, J.-M.; Sauvage, J.-P.; Hamann, C.; Palacin, S.; Bourgoin, J.-P. *Chem. Eur. J.* **2002**, *8*, 2153–2162. (d) Kaiser, G.; Jarroson, T.; Otto, S.; Ng, Y.-F.; Bond, A. D.; Sanders, J. K. M. *Angew. Chem., Int. Ed.* **2004**, *43*, 1959–1962. (e) Fuller, A. M. L.; Leigh, D. A.; Lusby, P. J.; Slawin, A. M. Z.; Walker, D. B. *J. Am. Chem. Soc.* **2005**, *127*, 12612–12619. (f) Leigh, D. A.; Lusby, P. J.; Slawin, A. M. Z.; Walker, D. B. *Angew. Chem., Int. Ed.* **2005**, *44*, 4557–4564.
- (4) (a) Li, X.; Liu, D. R. *Angew. Chem., Int. Ed.* **2004**, *43*, 4848–4870. (b) Diederich, F.; Stang, P. J., Eds. *Templated Organic Synthesis*; Wiley-VCH: Weinheim, 2000. (c) Aricó, F.; Badjic, J. D.; Cantrill, S. J.; Flood, A. H.; Leung, K. C.-F.; Liu, Y.; Stoddart, J. F. *Top. Curr. Chem.* **2005**, *249*, 203–259.
- (5) (a) Otto, S.; Furlan, R. L. E.; Sanders, J. K. M. *Science* **2002**, *297*, 590–593. (b) Krishnan-Ghosh, Y.; Balasubramanian, S. *Angew. Chem., Int. Ed.* **2003**, *42*, 2171–2173. (c) Leclaire, J.; Vial, L.; Otto, S.; Sanders, J. K. M. *Chem. Commun.* **2005**, 15, 1959–1961. (d) Hioki, H.; Still, W. C. *J. Org. Chem.* **1998**, *63*, 904–905. (e) Otto, S.; Furlan, R. L. E.; Sanders, J. K. M. *J. Am. Chem. Soc.* **2000**, *122*, 12063–12064. (f) Corbett, P. T.; Sanders, J. K. M.; Otto, S. *J. Am. Chem. Soc.* **2005**, *127*, 9390–9392. (g) Corbett, P. T.; Tong, L. H.; Sanders, J. K. M.; Otto, S. *J. Am. Chem. Soc.* **2005**, *127*, 8902–8903.
- (6) Wang, W.; Wang, L. Q.; Palmer, J.; Exarhos, G.; Li, A. D. Q. *J. Am. Chem. Soc.* **2006**, *128*, 11150–11159.
- (7) Han, J. J.; Shaller, A. D.; Li, A. D. Q. *J. Am. Chem. Soc.* **2008**, *130*, 6974–6982.

**Scheme 1.** Synthesis of Chiral, Twisted Monomers as the Starting Material for Diastereomeric Dimers<sup>a</sup>

<sup>a</sup> Only the *R* isomer is shown for clarity.

effects.<sup>8,9</sup> We also demonstrated linear perylene oligomers from dimer through 11-mer spontaneously fold and remain folded in  $\pi$ -stacks, even at nanomolar concentrations.<sup>7,8,10</sup> Next, we exhibited that dynamic self-assembly (DSA) effectively directs and enhances specific reaction pathways, employing weak  $\pi$ -stacking interactions to self-template specific covalent bond formation.<sup>6</sup>

In this paper, we expand the self-assembly and folding knowledge base by examining the role of molecular recognition between chiral aromatic systems. Known highly twisted (37°),<sup>11</sup> chiral,<sup>12</sup> bay-substituted tetrachloro-PDI monomers were used as the building blocks to synthesize diastereomeric linear and cyclic dimers. The cyclic diastereomeric dimers are separable by HPLC and stable at low temperatures, but they slowly interconvert at room temperature. Dimer characterization reveals that the preferred self-assembly, hereafter called the molecular code, effectively directs the coupling reaction pathway, favoring distinct homochiral and heterochiral structures. Solvophobic-driven folding is distinguished between the unique dimers, deciphering an inherent chiral molecular code between twisted PDIs that directs the resulting molecular architectures.

## Experimental Procedures

The syntheses of the cyclic and linear dimers and their intermediates are detailed in the Supporting Information. Solvents and reagents were purified where necessary using literature methods. MALDI-TOF mass spectra were obtained with an ABVS-2025 spectrometer. Electrospray ionization (ESI) mass spectra were obtained with an API-4000 triple-quadrupole spectrometer. <sup>1</sup>H, <sup>13</sup>C, and <sup>31</sup>P NMR spectra were recorded with a Mercury 300 (300 MHz) spectrometer in CDCl<sub>3</sub> (CD<sub>3</sub>OD) solutions. Bruker 500 and 600 MHz NMR spectrometers were also used whenever necessary. Absorbance spectra were recorded with a Varian Cary 100

spectrophotometer. Fluorescence spectra were recorded with a SPEX Fluorolog-3-21 spectrofluorometer with excitation at 489 nm. Reactions were monitored by thin-layer chromatography (TLC) on a precoated plate of silica gel 60 F254 (EM Science). Column chromatography was performed on silica gel 60 (230–400 mesh, EM Science). HPLC was performed with an Agilent 1100 series instrument using a normal-phase column and CH<sub>2</sub>Cl<sub>2</sub>/MeOH eluent.

## Results and Discussion

**Monomer Synthesis.** We incorporated flexible TEG chains to provide the linkages between the rigid perylene cores, in contrast to numerous other PDI derivatives reported with various imide functional groups.<sup>12–14</sup> More rigid or sterically demanding groups such as 2,6-diisopropylaniline, swallowtail alkyl chains, or 3,4,5-trialkyl-substituted aniline groups are designed in part to prevent aggregation, an obvious advantage for design of highly fluorescent pigments, light harvesting arrays, and highly fluorescent dendrimers. However, these diminish the desired unique self-assembly properties responsible for molecular codes. The TEG chains afford high solubility in common chlorinated solvents while minimally retarding the  $\pi$ - $\pi$  stacking properties of the perylene core. They also facilitate simple, robust, and high-yield coupling reactions such as the disulfide and phosphoramidite strategies applied here.

Scheme 1 outlines the synthesis of the monomeric starting material for the diastereomeric cyclic dimers. Tetrachloro-substituted perylenetetracarboxylic acid was synthesized according to a literature procedure,<sup>15</sup> as were the amino-functionalized TEG chains,<sup>10</sup> which were attached to both ends of the twisted perylene core as imides **1**. The significantly increased solubility of the highly twisted core allows the reaction to proceed in the easily removed solvent pyridine rather than higher boiling point solvents such as dimethylsulfoxide or quinoline required for the planar unsubstituted perylene. The chain-end hydroxyl groups in **1** were tosylated to yield **2**,

(8) Wang, W.; Han, J.; Wang, L.-Q.; Li, L.-S.; Shaw, W.; Li, A. D. Q. *Nano Lett.* **2003**, *3*, 455–458.

(9) Li, A. D. Q.; Wang, W.; Wang, L. Q. *Chem. Eur. J.* **2003**, *9*, 4594–4601.

(10) Wang, W.; Li, L.-S.; Helms, G.; Zhou, H.; Li, A. D. Q. *J. Am. Chem. Soc.* **2003**, *125*, 1120–1121.

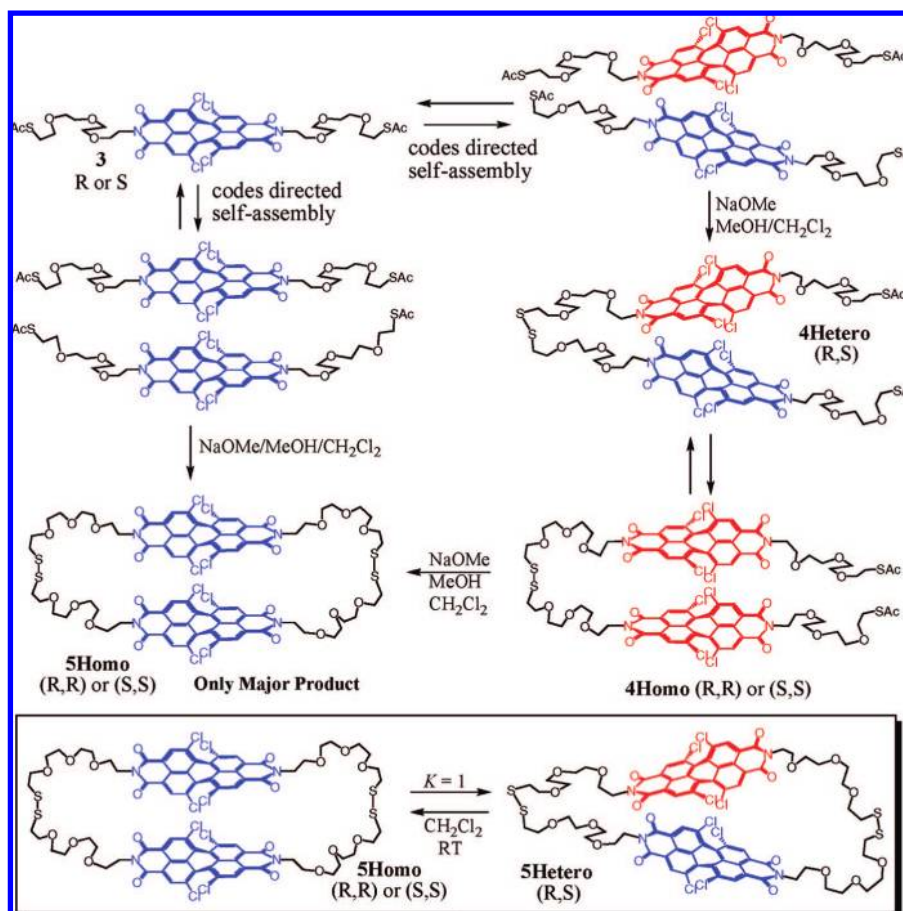
(11) Chen, Z.; Debiji, M.; Debaerdemaeker, T.; Osswald, P.; Würthner, F. *Chem. Phys. Chem.* **2004**, *5*, 137–140.

(12) Osswald, P.; Würthner, F. *J. Am. Chem. Soc.* **2007**, *129*, 14319–14326.

(13) Zhang, X.; Chen, Z.; Würthner, F. *J. Am. Chem. Soc.* **2007**, *129*, 4886–4867.

(14) Klok, H.-A.; Becker, S.; Schuck, F.; Pakula, T.; Mullen, K. *Macromol. Biosci.* **2003**, *3*, 729–741.

(15) Rogovik, V.; Gutnik, L. *Zh. Org. Khim.* **1988**, *24*, 635–639.

Scheme 2. Synthesis of Diastereomeric Cyclic Dimers<sup>a</sup>

<sup>a</sup> Conditions: NaOMe/MeOH, open to air at room temperature;  $H^+$  quench to stop the reaction. The chiral monomer **3** (*R* or *S* enantiomer) creates two molecular codes: the homochiral assembly (*R-R* or *S-S*) and the heterochiral assembly (*R-S*). These dynamic self-assemblies effectively direct the formation of cyclic dimer product **5Homo** (*R,R* or *S,S* enantiomers) and intermediate heterochiral linear dimer **4Hetero**. No heterochiral cyclic dimer is formed. The homochiral cyclic dimer **5Homo**, however, slowly interconverts to the meso heterochiral cyclic dimer **5Hetero** (*R,S*) at room temperature, until reaching a 50/50 mixture.

followed by substitution of the tosyl groups with thiol acetate groups to form the dithioacetate **3**, the cyclization reaction starting material.

**Diastereomeric Cyclic Dimers.** Disulfide chemistry was used to form the cyclic dimers, a recognized ring-closure strategy where disulfide linkages are readily triggered by air oxidation under basic deacetylation conditions.<sup>2d,5</sup> We have reported this chemistry in detail previously, demonstrating that various ring structures are formed from planar perylene monomers, resulting in dimer rings, concatenated tetramer rings, or monomeric rings, depending on the monomer concentration and reaction time.<sup>6</sup> Since twisting the perylene core imparts chirality, dynamic self-assembly effectively sorts out and directs enantiomerically pure organization. This indicates that molecular size, shape, and electric potential distributions function like specific codes that can be exploited to benefit specific products.

The strategy to form cyclic dimers is outlined in Scheme 2. Deacetylating a racemic mixture of the twisted chiral monomer **3** initially yielded the homochiral cyclic product **5Homo** and the heterochiral linear dimer **4Hetero**, as indicated by TLC. Quenching the reaction early captured these two products, which were separated by column chromatography and characterized by NMR and mass spectrometry. When the reaction was allowed to proceed to completion, **5Homo** was the only main product. Unlike the achiral planar monomers, no concatenated or

monomer-ring compounds were detected. Interestingly, very little heterochiral cyclic dimer **5Hetero** was detected during the reaction. Upon standing, however, **5Homo** spontaneously, albeit slowly, equilibrated with its heterochiral diastereomer **5Hetero** at room temperature, until their ratio reached 1:1 after 24 h.

It is instructive to compare the achiral planar molecules to the twisted chiral monomers. The planar perylene readily  $\pi$ -stacks with other planar monomers, forming a self-assembled structure favorable for cooperative disulfide-bond formation and cyclic products. This hypothesis was validated previously because no reactive intermediates were observed, regardless of how fast the reaction was quenched. The twisted chiral molecules, however, have two options: homo template (*R-R* or *S-S*  $\pi$ -stack) or hetero template (*R-S*  $\pi$ -stack). Obviously, the homo template and the hetero template have different self-assembled structures and thus control the reaction pathway differently, although both reactions are accelerated by the self-assembly effect.

Our experimental results reveal that the homo template directs cooperative disulfide-bond formation, yielding a cyclic dimer, **5Homo**, whereas the hetero template endures a stepwise reaction, first producing a linear heterodimer, **4Hetero**. This linear heterodimer equilibrates with its counterpart, the linear homodimer **4Homo**, which then folds according to the homo template molecular code rather than hetero template molecular

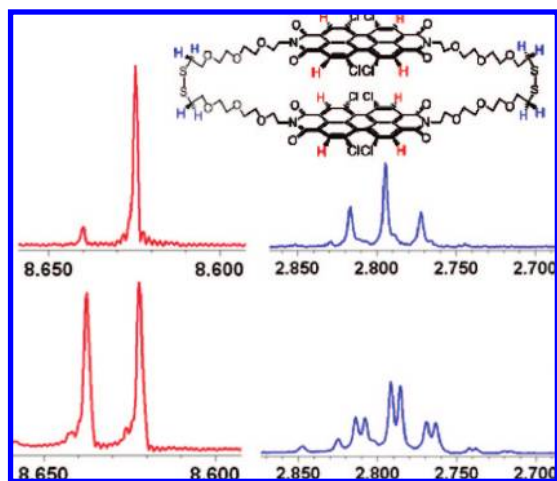


**Figure 1.** NMR spectra recorded during the isomerization reaction. (Top) **5Homo** exhibits one peak for all eight identical aromatic protons (left, red) and only one triplet for protons adjacent to the disulfide bonds (right, blue). (Bottom) **5Homo** interconverts to **5Hetero**, reaching a 50/50 diastereomeric mixture in about 24 h. The mixture then exhibits two equally integrated perylene peaks and two equal triplets for protons adjacent to the disulfide. Solvent:  $\text{CDCl}_3$ .

code. Since homo template molecular code favors the reaction pathway toward homocyclic formation, **4Homo** is converted to the cyclic homodimer **5Homo**. The cyclization of the homodimer effectively removes it from the equilibrium, causing more **4Hetero** to convert to **4Homo** (Le Chatelier's principle). Thus, the conversion rate is greatly increased when compared to cyclic dimer interconversion.

Why did the twisted-monomer reaction yield no measurable concatenated rings? According to our concatenation mechanism, the cyclic dimer and linear monomer template reacting with another linear monomer simultaneously produced concatenated rings. Planar perylene derivatives have identical intercomplementary molecular codes. The twisted perylene derivatives, however, are different: the racemic mixture creates two molecular codes. A concatenated tetramer prefers *R,R,R,R* or *S,S,S,S* configurations sterically. The probability of forming such a homochiral tetramer is only 1/8 of planar concatenated rings because homodimers and linear monomers have only 1/2 probability of participating in the reaction for a racemic mixture. In addition, steric hindrance probably further discourages the formation of such a template in twisted structures that leads to concatenated rings. These analyses reduce the theoretical yield of the concatenated rings to less than a few percent, a level difficult to isolate.

**Cyclic Homo- and Heterodimer Equilibrium.**  $^1\text{H}$  NMR first revealed the equilibrium between the homo- and heterochiral dimers, which are diastereomers. On the NMR time scale, **5Homo** exists as a pair of enantiomers (*R,R* and *S,S*) with  $D_2$  symmetry, while **5Hetero** is a meso compound (*R,S*) with  $C_{2h}$  symmetry (Figure 1, Supporting Information). Thus, both diastereomers have a single peak representing all eight aromatic protons, although the peaks are slightly different for the two compounds. Similarly, the TEG chain protons also experience slightly different chemical shifts between the diastereomeric pair; the protons directly adjacent to the disulfide bonds are conveniently well resolved from other peaks and particularly sensitive to isomerization. Immediately following reaction quenching, **5Homo** was purified and characterized by NMR, showing mainly one aromatic peak and a single triplet for the disulfide-

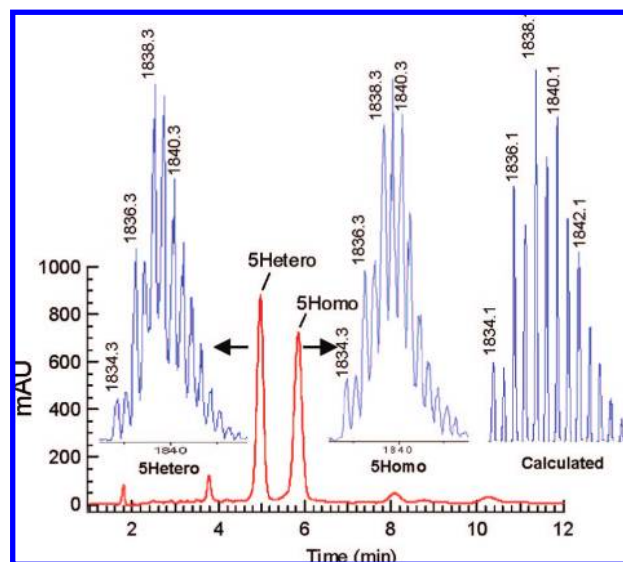


**Figure 2.** Normal-phase HPLC spectra of **5Homo** and **5Hetero**, showing that **5Hetero** elutes first. The fractions collected were immediately characterized by ESI. Inset: Nearly identical mass spectra were obtained for **5Hetero** (left) and **5Homo** (right), closely matching the calculated isotopic pattern, with the exact  $m/z$  for  $[\mathbf{5Homo} + \text{NH}_4]^+ = [\mathbf{5Hetero} + \text{NH}_4]^+ = 1834.1$ .

adjacent protons (Figure 1, top). However, upon allowing the purified **5Homo** solution to equilibrate in  $\text{CH}_2\text{Cl}_2$  for >24 h, two aromatic peaks with equal integration were apparent, and the disulfide-adjacent protons displayed two equal-sized overlapping triplets concomitantly (Figure 1, bottom). The first reaction product generates the higher field aromatic peak, has a lower chromatographic  $R_f$ , and has a lower  $A^{0-0}/A^{0-1}$  absorbance ratio (vide infra), consistent with greater  $\pi-\pi$  overlap. Modeling shows the homo structure has a larger overlap than the hetero one; thus, we assign the product as **5Homo**.

To determine if the two compounds were truly interconverted diastereomers, we used normal-phase HPLC to separate and purify the suspected isomers. The compounds separated surprisingly well, with **5Hetero** eluting before **5Homo** because of the more steric and soluble hetero structure (Figure 2). The separate fractions were collected and immediately characterized by ESI mass spectrometry; each compound exhibited almost identical mass and isotopic distributions, consistent with the cyclic dimer containing eight chlorine atoms (Figure 2).

We then performed HPLC monitoring, starting with each purified compound at room temperature, to examine if the diastereomers truly interconvert, or if the conversion proceeds in only one direction (Figure 3). Convincingly, the reaction proceeded in both directions until reaching a 50/50 mixture in about 24 h, after which no further change in ratio occurred. Noticing the relative slow interconversion rate, we next examined the temperature dependence of the isomerization reaction rate. When a solution of **5Hetero** in  $\text{CDCl}_3$  was maintained at  $-20^\circ\text{C}$  for 24 h, NMR proved that no noticeable isomerization occurred (Figure 4). These results are consistent with our own studies<sup>16</sup> and the recently reported free energy barrier of 87 kJ/mol for interconverting chiral twisted tetrachloroperylene enantiomers.<sup>11</sup>

**Self-Assembly Functions as Molecular Codes.** The absence of concatenated rings suggests that the *twisted* tetrachloro-

(16) Wang, W.; Bain, A. D.; Wang, L.-Q.; Exarhos, G. J.; Li, A. D. Q. *J. Phys. Chem. A* **2008**, *112*, 3094–3103.

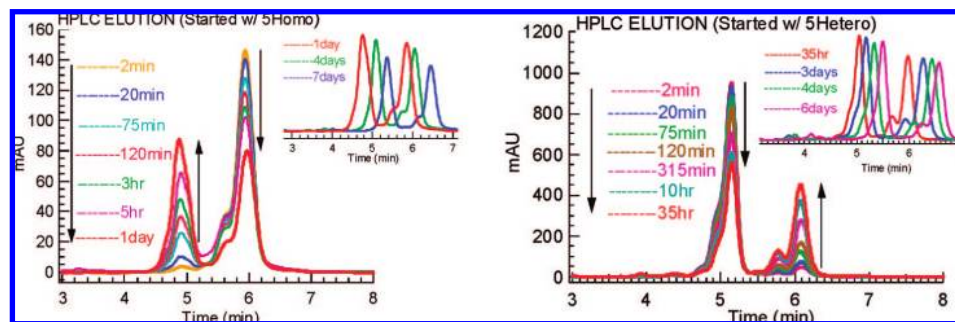


**Figure 3.** HPLC spectra recorded during the isomerization reaction. Pure **5Homo** (left) or **5Hetero** (right) interconverts to its isomers at room temperature in  $\text{CH}_2\text{Cl}_2$ . The reaction proceeds in both directions until reaching a 1:1 equilibrium in about one day. Inset: Longer reaction time monitoring still showed 1:1 mixtures after several days (peaks shift to longer elution times due to change in solvent polarity).

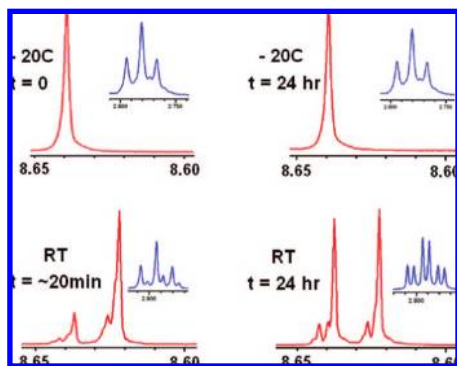


**Figure 4.** (Top) NMR spectra recorded after a solution of **5Hetero** in  $\text{CDCl}_3$  was maintained at  $-20^\circ\text{C}$  for 24 h. No noticeable isomerization occurred. (Bottom) NMR spectra recorded after a solution of **5Homo** was left at room temperature for 24 h. A significant amount of **5Hetero** was formed. Triplets for disulfide adjacent protons are inset for each sample.

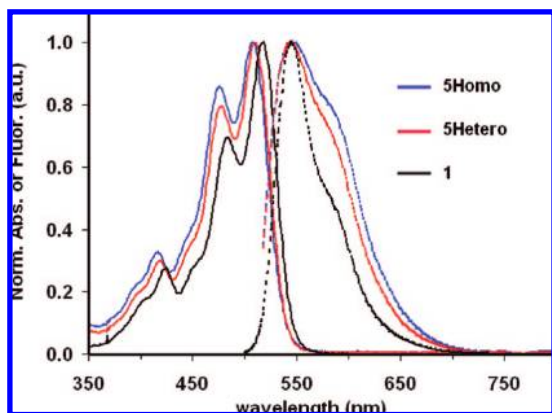


**Figure 5.** Absorbance (solid lines) and fluorescence (dashed lines) spectra recorded in  $\text{CH}_2\text{Cl}_2$  for **5Homo** (blue) and **5Hetero** (red) compared to the monomer **1** (black). A lower  $A^{0-0}/A^{0-1}$  ratio for the homochiral dimer (1.18) than for the heterochiral dimer (1.28) indicates a slight difference in packing structures. Fluorescence  $F^{0-0}/F^{0-1}$  ratios corroborate the absorbance Franck–Condon factors.

erylene units impart an effect on reaction pathways, favoring disulfide-bond formation leading exclusively to cyclic dimers. Conversely, *planar* monomers do not have such an effect, and the reaction proceeds to concatenation in high yield.<sup>6</sup> Thus, if stacks greater than two *twisted* monomers form, they must be oriented in such a way that only disulfide bonds between adjacent monomers are favorable. The *planar* perylene, however, was oriented in such a way that alternating members of the stack could react, forming concatenated rings. Ab initio and DFT calculations consistently predict that stacked adjacent *planar*

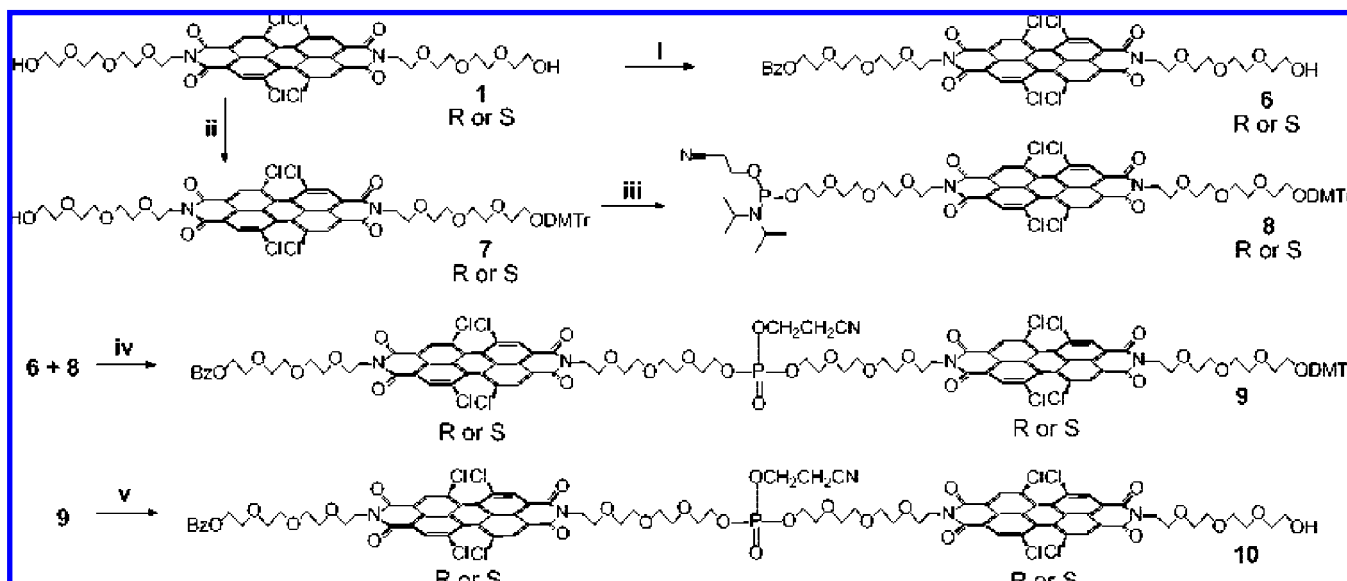
perylene are probably rotated  $30^\circ$  from each other, separated by  $3.5 \text{ \AA}$ .<sup>17</sup> Thus, alternating stack members may be rotated  $60^\circ$  from each other or oriented in parallel, perfect for cooperative catenation. The twisted tetrachloro units apparently preclude this rotational ambiguity, forcing thiol group orientation to be unfavorable for disulfide-bond formation between any units other than those directly adjacent to each other.

At low concentrations (and thus limited self-assembly template effect), the *planar* perylene forms a monocyclic ring,<sup>6</sup> while the highly *twisted* monocyclic tetrachloroperylene does not. One possible explanation for the absence of *twisted* monocyclic tetrachloroperylene ring formation is that the twist angle separates the two thiol groups unfavorably for intramolecular disulfide-bond formation. As the two naphthalene planes are twisted closer to perpendicular, the idealized zigzag TEG chains also become perpendicular to each other, rendering lower intramolecular reaction probability between the two sulfur atoms. Experimentally, NMR has shown that the ethylene unit connected to the diimide is relatively more rigid than the other ethylene units,<sup>16</sup> and therefore twisting the perylene core coupled to the first rigid ethylene unit abates the probability of forming an intramolecular disulfide bond. The added steric hindrance of the four chlorine atoms is not likely responsible, as the much bulkier, moderately twisted tetraphenoxyperylene ( $\theta \approx 25^\circ$ ) readily forms the monocyclic structure.<sup>16</sup> Unless there are distinguishing electronic effects between the reactive thiol groups and the  $\text{Cl}_4$ -perylene core, the orientation steering is a reasonable explanation.

The most remarkable result of the twisted cyclization reaction is that only homochiral cyclic dimers form directly and exclusively from the monomer racemic mixture. The perylene units first undergo molecular recognition, dynamically self-assembling conducive to subsequent disulfide-bond formation. Homochiral assembly directs nearly *simultaneous* disulfide-bond formation leading directly to cyclic **5Homo**, whereas heterochiral assembly directs *stepwise* disulfide coupling via intermediate linear **4Hetero**, precluding heterocyclization.

If instead the first disulfide bond formed primarily by random *intermolecular* collision without self-assembly directing effects, the second disulfide bond must similarly form by random *intramolecular* collision. Generally, intramolecular reactions are greatly accelerated over intermolecular reactions due to reduced activation entropy. However, **4Hetero** never directly cyclizes, while **4Homo** is never isolated because it rapidly proceeds to **5Homo**. What prevents **4Hetero** from cyclizing? In the absence

(17) Clark, A.; Qin, C.; Li, A. D. Q. *J. Am. Chem. Soc.* **2007**, *129*, 7586–7595.

Scheme 3. Synthesis Route to the Foldable Dimer<sup>a</sup>

<sup>a</sup> Conditions: (i) benzoyl chloride/py; (ii) 4,4'-dimethoxytrityl chloride, DMAP/py; (iii) 2-cyanoethyl-*N,N*-diisopropylchlorophosphoramidite, diisopropylethylamine/DCM; (iv) NPhIMT, DCM, then I<sub>2</sub> (DCM/Py/H<sub>2</sub>O 1:3:1), room temperature; (v) TCA/DCM, room temperature.

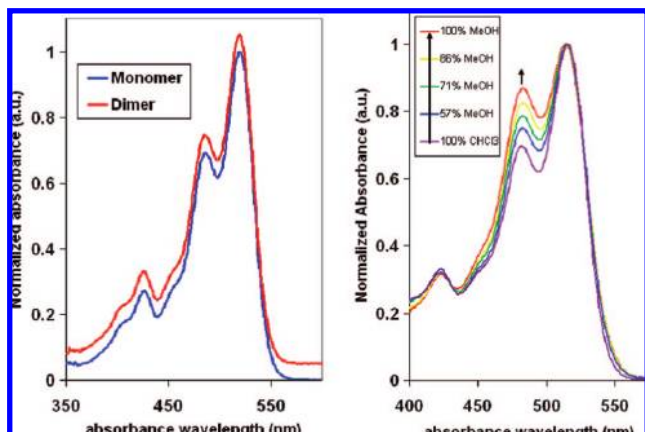


**Figure 6.** (Left) Comparison of dimer absorbance and monomer absorbance in pure chloroform. The dimer is slightly vertically off-set for clarity. (Right) Absorbance spectra monitoring the linear dimer folding in chloroform/methanol gradient. Methanol increases the solvophobicity, causing the dimer to fold, resulting in a diagnostic increase in the ratio  $A^{0-0}/A^{0-1}$  of the vibronic bands. In pure chloroform the ratio is 1.43, while in pure MeOH the ratio is 1.15. This ratio for the monomer does not change even in pure methanol (not shown).

of molecular codes, steric hindrance between heterochiral perylene units could conceivably discourage favorable *S-S* contact. However, modeling shows minimal differences between **4Homo** and **4Hetero** in intramolecular steric resistance, leaving many other available configurations with likely intramolecular thiol collision probability. This is supported by a nearly temperature independent  $K_{eq} \approx 1$  for the interconversion between **5Homo** and **5Hetero**, revealing that the hetero template is similarly favored thermodynamically over the homo template. Had the cyclization been mainly governed by the free energy difference between hetero and homo perylene stacking, **4Homo** and **4Hetero** would equally cyclize to yield **5Homo** and **5Hetero**, respectively, because they have the same free energy in the stacked states ( $G_{5Homo} = G_{5Hetero}$ ). Thus, a random intramolecular collision between thiols would be nearly equally favored in each case, and the reaction product would be a 1:1

ratio of **5Homo** to **5Hetero**. Because **5Hetero** is not a reaction product, intramolecular assembly must precede cyclization, where the folded **4Hetero** structure unfavorably orients the remaining thiols, effectively blocking the reaction. Thus, molecular codes control such reactions. The same code responsible for intramolecular folding must also direct intermolecular self-organization, as the molecular code is not selectively turned on and off. What hetero configuration could cause such an unfavorable orientation? Modeling shows that longitudinally offset stacking or perpendicular cofacial rotation could greatly reduce the likelihood of the 90°–90° offset elbow C–S–S–C bond formation. Regardless, the appearance of strictly heterochiral linear dimers and homochiral cyclic dimers elucidates unique molecular codes.

The code phenomenon can be explained as follows: Weak,  $\pi$ -stacking force brings the monomers together via dynamic self-assembly. (The self-assembly enthalpy  $\Delta H_{SA}$  was determined to be  $-3-7$  kcal/mol in the *planar* units<sup>8,9</sup> and smaller in the *twisted* units.) Negative  $\Delta H_{SA}$  helps compensate the self-assembly entropy  $\Delta S_{SA}$  (also negative), thus bringing some perylene units within 3.5 Å of each other, a favorable reaction environment. The efficaciously reduced assembly entropy pays at least partially the disulfide-bond activation entropy penalty,  $\Delta S_{S-S}^{\ddagger}$ . The perylene template locates the TEG chain ends near each other so that the thiol reactive intermediates can react favorably to form disulfide bonds. Thus, the reaction rate is greatly increased, resulting in the kinetically favored homochiral cyclic dimer when the self-assembled monomers have complementary molecular codes. Heterochiral monomers also have a complementary molecular code; however, the heterochiral molecular code directs a different self-assembled structure, which leads to formation of the linear dimer rather than the cyclic dimer. If the molecular code is noncomplementary, such a specific reaction rate enhancement is absent.

Equation 1 shows the activation free energy that controls the reaction rate. To increase the rate, it is desired to make the disulfide-bond activation entropy  $\Delta S_{S-S}^{\ddagger}$  as close to zero as possible.  $\Delta S_{S-S}^{\ddagger}$  contains translational and orientation terms (eq 2), each of which the perylene self-assembly contributes to

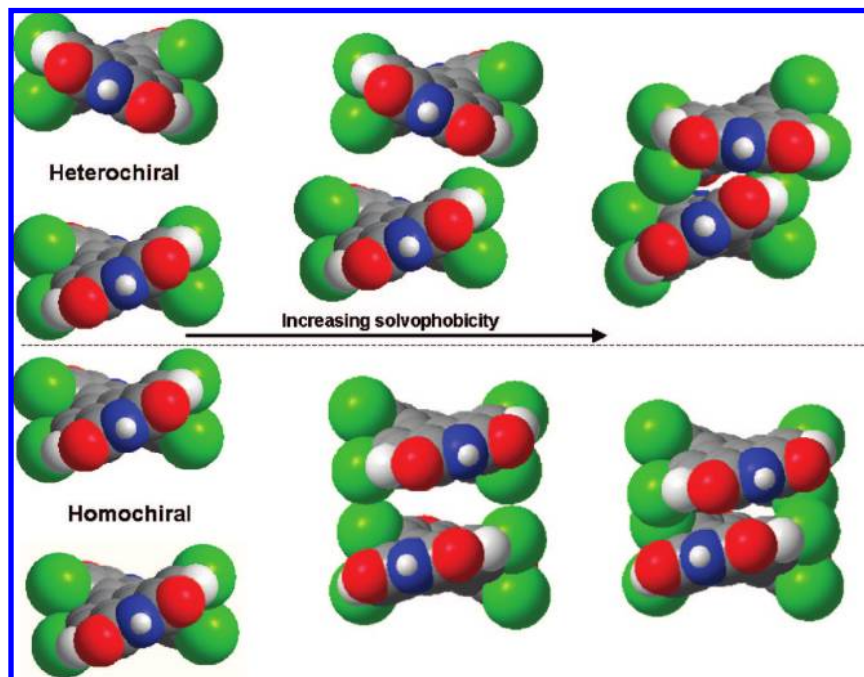


**Figure 7.** Merck Molecular Force Field (MMFF94) energy-minimized models, contrasting possible folded configurations in the heterochiral dimer (top) and the homochiral dimer (bottom) with increasing solvophobicity. As solvophobic forces drive the dimer to fold, molecular recognition codes different homo- and heterochiral structures. Ultimately, the homochiral dimer stacks with greater  $\pi$ - $\pi$  overlap. All atoms except for the perylene core are omitted for clarity.

improving. The translational entropy penalty,  $T\Delta S_{S-S, \text{translation}}^{\ddagger}$ , depends on the concentration but typically is  $-(8-10)$  kcal/mol at 1 M, while the orientation penalty,  $T\Delta S_{S-S, \text{orientation}}^{\ddagger}$ , is typically  $-(3-8)$  kcal/mol.<sup>18</sup> Dynamic self-assembly reduces the number of independent molecules, with a consequent loss of three translational and up to three rotational degrees of freedom, albeit partially compensated by residual degrees of freedom in the self-assembled structure, especially in the flexible TEG chains. The perylene encounter complex likely provides catalytic factors of 2.4–6.0 kcal/mol, typical of other enzymic or chelate rate accelerations.<sup>18a</sup> Thus, self-assembly-induced diminishment in  $\Delta S_{S-S}^{\ddagger}$  significantly favors coded structure formation over random collision products.

$$\Delta G_{S-S}^{\ddagger} = \Delta H_{S-S}^{\ddagger} - T\Delta S_{S-S}^{\ddagger} \quad (1)$$

$$\Delta S_{S-S}^{\ddagger} = \Delta S_{S-S, \text{translation}}^{\ddagger} + \Delta S_{S-S, \text{orientation}}^{\ddagger} \quad (2)$$

The self-assembly-directed disulfide-bond formation is quasi-catalytic, but there is no catalyst by definition, as dynamic self-assembly is a phenomenon, not a substance. Catalysts are frequently associated with lowering the activation *enthalpy*, while activation *entropy* is often overlooked. The importance of activation enthalpy vs entropy is still highly debated; evidence supports that either entropy or enthalpy dominates the catalytic effect in many enzymes.<sup>19</sup> A popular alternative explanation is that self-assembly stabilizes the encounter complex, holding the transition-state thiol intermediates long enough to improve the

probability of proceeding to the disulfide.<sup>20</sup> Regardless of explanation, the self-assembly molecular code is significant, orchestrating unambiguous reaction pathways that yield distinct products.

**Spectroscopic Analysis.** We have previously demonstrated that perylene folding or self-organizing has a diagnostic indicator and changes the vibronic band ratio  $A^{0-0}/A^{0-1}$  in the absorbance spectrum.<sup>8,10</sup> Likewise, the Franck–Condon factor changes, as observed in the fluorescence spectrum, can also indicate similar interaction.<sup>8-10</sup> We have shown that *planar* cyclic and linear oligomers, when excited, form delocalized excited states, which have typical  $\pi$ -stack red emission, a tell-tale sign of  $\pi$  interactions.<sup>7,21</sup>

The **5Homo** and **5Hetero** absorbance and fluorescence spectra further reveal the nuance in the chiral molecular recognition code (Figure 5). The normalized spectra show that the diastereomers have a clear, noticeable difference in the  $A^{0-0}/A^{0-1}$  ratio. As expected, the homodimer ratio is lower than the heterodimer ratio because the homochiral rings have a larger  $\pi$ -stack area and a tighter fit, and thus they experience a greater displaced harmonic oscillator. The **5Homo** ratio is 1.18, while the **5Hetero** ratio is 1.28. Both cyclic dimers exhibit lower ratios than the monomer and the linear dimer; the monomer and linear dimer have a ratio of 1.43, indicating that the cyclic architecture imposes a considerable influence on the folding equilibrium. Interestingly, our previous report demonstrated that the linear and cyclic *planar* dimers were similarly folded, exhibiting  $A^{0-0}/A^{0-1}$  ratios of 0.84 and 0.73, respectively.<sup>7</sup> The highly twisted cores are reluctant to fold in the linear dimer but are architecturally forced to fold in the more structurally restrained cyclic dimers. The cyclic dimer  $\lambda_{\text{max}}$  are slightly hypsochromatically

(18) (a) Page, M.; Jencks, W. *Proc. Natl. Acad. Sci. U.S.A.* **1971**, *68*, 1678–1683. (b) Jenks, W. P. *Proc. Natl. Acad. Sci. U.S.A.* **1981**, *78*, 4046–4050. (c) Sugimura, T.; Hagiya, K.; Sato, Y.; Tei, T.; Tai, A.; Okuyama, T. *Org. Lett.* **2001**, *3*, 37–40. (d) Janin, J. *Proteins: Struct., Funct. Genet.* **1997**, *28*, 153–161.

(19) (a) Wolfenden, R.; Snider, M.; Ridgway, C.; Miller, B. *J. Am. Chem. Soc.* **1999**, *121*, 7419–7420. (b) Bruce, T.; Lightstone, F. *Acc. Chem. Res.* **1999**, *32*, 127–136. (c) Strajbl, M.; Sham, Y.; Villa, J.; Chu, Z.; Warshel, A. *J. Phys. Chem. B* **2000**, *104*, 4578–4584.

(20) Frisch, C.; Fersht, A.; Schreiber, G. *J. Mol. Biol.* **2001**, *308*, 69–77.

(21) Han, J. J.; Wang, W.; Li, A. D. Q. *J. Am. Chem. Soc.* **2006**, *128*, 672–673.

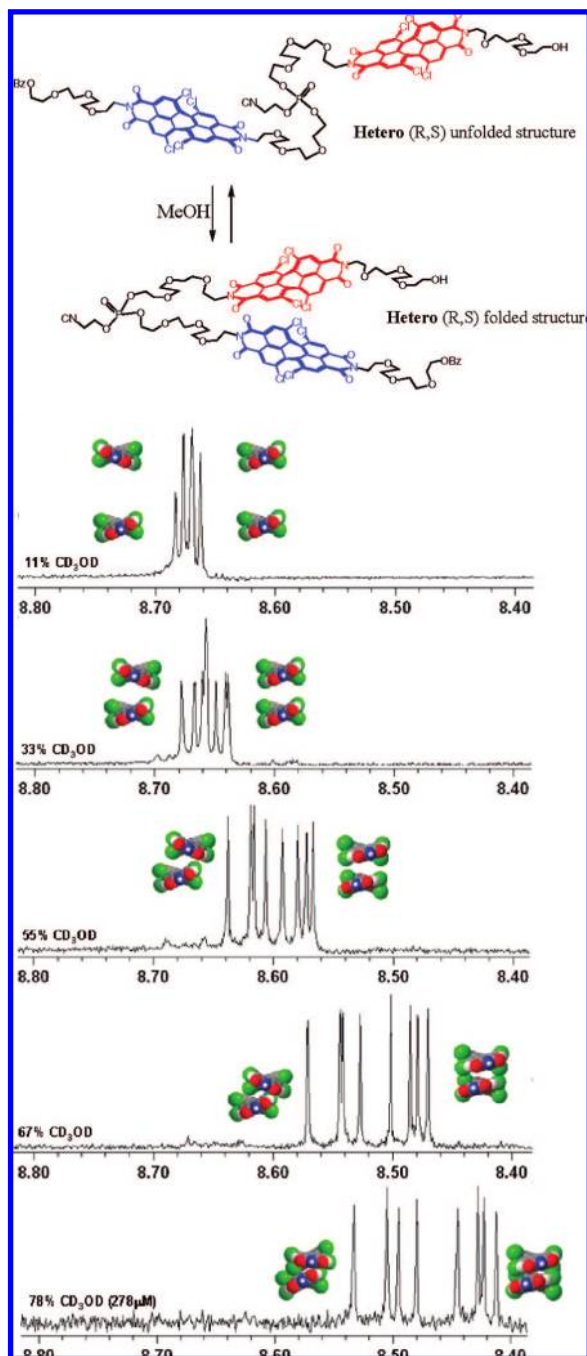


**Figure 8.** (Top) Scheme showing solvent-dependent folding equilibrium for the heterochiral linear dimer. (Bottom)  $^1\text{H}$  NMR spectra of the foldable linear dimer recorded while varying the  $\text{CDCl}_3/\text{CD}_3\text{OD}$  gradient;  $\text{CD}_3\text{OD}$  percentage is listed for each spectrum. Increasing the solvophobicity with methanol causes the dimer equilibrium to increase, resulting in a stronger ring-current effect and a concomitant upfield chemical shift. The homochiral dimers ( $R,R$  and  $S,S$ ) and heterochiral dimers ( $R,S$  and  $S,R$ ) have distinct folded structures, as evidenced by different chemical resonances. The first four spectra are taken at 1.4 mM; the last spectrum is recorded at 278  $\mu\text{M}$  to maintain solubility. Maintenance of symmetric peak structure limited to upfield chemical shift emphasizes that the folding equilibrium is dynamic and fast on the NMR time scale.

shifted from that of the free monomer, a further indication of folding interactions.

The fluorescent spectrum also shows subtle differences in the Franck–Condon factors, which again indicates a more slightly displaced harmonic oscillator in the homochiral dimer. Unlike the *planar* dimers,  $\pi$ -stack red emission is not observed in the

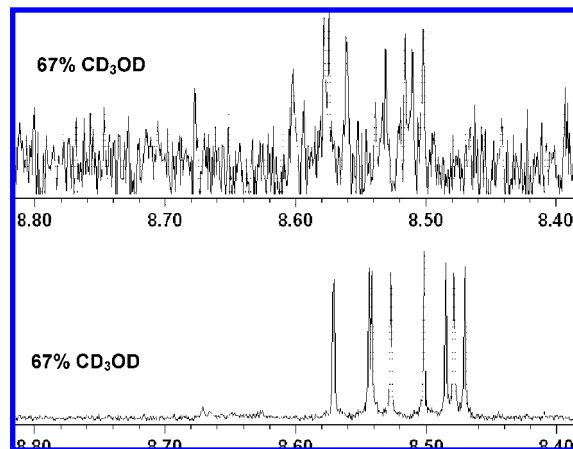


**Figure 9.**  $^1\text{H}$  NMR spectra of a control experiment in which the dimer concentration was varied from 27.8  $\mu\text{M}$  to 1.389 mM (limit of solubility) while maintaining a constant 67% methanol concentration. The high-concentration sample shifted by only 0.03 ppm upfield when compared to the low-concentration sample, demonstrating that most chemical resonance shifts are due to intramolecular folding effects and not intermolecular self-assembly.

twisted dimers, indicating no delocalized excited states. Thus, while the vibronic band ratios indicate ground-state interaction, the excited-state coupling strength between adjacent chromophores must be too weak to establish delocalization.

**Foldable Linear Dimer.** To complement the cyclic ring chemistry, the twisted tetrachloro-erylene and its chirality-responsive folding were investigated using a different approach. The new approach uses a phosphotriester linkage to replace the exchangeable disulfide bond to form a linear *foldable* dimer. Scheme 3 outlines the synthesis strategy.

The dynamic folding equilibrium constant  $K_{\text{fold}}$  for the dimer **10** remains small in chlorinated solvents such as chloroform because the highly twisted perylene has tuned down the  $\pi$ -stacking force, apparent in the absorbance spectra where the  $A^{0-0}/A^{0-1}$  vibrational peak ratio remains nearly the same as for the monomer (Figure 6, left). This is in contrast to the more architecturally restrained cyclic dimer, which exhibits considerable folding in chlorinated solvents. However, increasing the methanol concentration generates solvophobicity, and  $K_{\text{fold}}$  increases as the diagnostic  $A^{0-0}/A^{0-1}$  vibronic band ratio grows (Figure 6, right). In pure chloroform the ratio is 1.43, while in pure MeOH the ratio is 1.15. The *monomer* ratio does not change at these low concentrations prepared for absorbance measurements, even in pure methanol ( $\ll$ critical concentration).

Although not apparent from the UV/vis spectrum, the diastereomers begin to differentiate themselves as their molecular recognition codes begin to enforce compatibility (Figure 7). The homochiral dimers ( $R,R$  and  $S,S$ ) are not as sterically frustrated as the heterochiral dimers ( $R,S$  and  $S,R$ ), and thus they experience a slightly more negative enthalpy of folding. As hinted early, the homo molecular code has a different structure than the hetero molecular code; NMR should be able to distinguish the linear folded homodimer and heterodimer.

Ultimately, the homochiral dimer is able to fold with a greater  $\pi$ - $\pi$  overlap for a given solvent composition and can be detected by NMR. The *cyclic* tetrachloro perylene  $R,R$  ( $S,S$ ) or  $R,S$  compound has only one equivalent aromatic proton due to symmetric configurations, each showing a distinct chemical shift (*vide supra*). However, the *linear* foldable dimer has a benzoyl anchor on one end and a hydroxyl group on the other and

therefore has four separate aromatic protons for each of the homodimers and the heterodimers. The unfolded linear dimer chemical shifts have aromatic proton resonances similar to that of **4Hetero** ( $\sim 8.67$  ppm) as long as the concentration is below the critical self-assembly concentration (about 10 mM).

However, increasing the solvophobicity forces the dimers to fold, inducing an upfield chemical shift of the aromatic protons. As the methanol concentration increases, homochiral dimer folding has a larger  $\pi$ -contact area, and the aromatic protons experience a greater upfield chemical shift as a result of the ring current. Thus, similar to those of the cyclic dimers, the linear homodimer peaks are farther upfield than the linear heterodimer peaks.

The homo- and heterochiral dimer mixtures were diluted to the same concentration (1.4 mM) using various ratios of deuterated chloroform and methanol. The NMR spectra were recorded at room temperature and the perylene core aromatic proton chemical shifts compared (Figure 8). At 11% methanol (v/v), the homo- and heterodimers, adopting mostly the unfolded configuration, exhibit identical chemical shifts, both displaying four sharp peaks in a narrow 0.020-ppm region. As the concentration of methanol is increased to 33%, the peaks begin to differentiate. At just over 50% methanol concentration, the diastereomers are completely resolved, and eight sharp peaks are clearly visible. At 66% methanol, the high-field stereoisomer and the low-field stereoisomer are separated by as much as 0.099 ppm.

To see how far the diastereomers could be differentiated, a lower concentration (278  $\mu\text{M}$ ) was prepared, allowing solubility in 78% methanol. In this case, the difference between the isomers increased to 0.120 ppm, clearly separating the proton groups belonging to homodimers from those of heterodimers.

Since increasing the solvophobicity can also decrease the critical self-assembly concentration and ultimately lead to intermolecular interactions, a control experiment was performed at a constant 67% methanol concentration while varying the dimer concentration from 28  $\mu\text{M}$  to 1.4 mM (limit of solubility). Over this broad concentration range, the two isomers produce a chemical shift difference of only  $\sim 0.03$  ppm (Figure 9), demonstrating that most of the chemical shift differentiation is due to intramolecular folding effects and not intermolecular self-assembly.

## Conclusion

We have synthesized both cyclic and linear diastereomeric dimers using highly twisted tetrachloroperylene monomers to impart chirality and molecular codes. The homochiral self-assembly directs a cooperative reaction, resulting in both disulfide bonds forming nearly simultaneously to yield the cyclic dimer, **5Homo**, whereas the heterochiral self-assembly directs

a stepwise reaction, leading to one disulfide-bond formation and the corresponding linear dimer, **4Hetero**. These observations provide convincing insight into how self-assembly can function as molecular codes that direct reaction pathways. Only homochiral cyclic dimers are formed from twisted chiral monomers, providing strong evidence that self-assembly precedes ring formation and there is a preferred molecular homochiral recognition code. The self-assembly template directs ring formation, likely by reducing the disulfide-bond activation entropy penalty and favorably orienting the free-standing thiol groups into juxtaposed positions to increase the kinetic rate of disulfide-bond formation.

The homochiral cyclic dimers spontaneously interconvert to the heterochiral cyclic dimer at room temperature, reaching a 1:1 equilibrium in  $\sim 24$  h. However, heterochiral cyclic dimer cannot be synthesized directly from the racemic monomer mixture because of forbidden molecular codes. To summarize, the homocyclic dimer is kinetically favored; however, the kinetic product eventually reaches a 1:1 equilibrium with its thermodynamically equally favored diastereomer.

A complementary diastereomeric linear dimer was synthesized using phosphoramidite chemistry to study the solvent-dependent folding equilibrium. In contrast to the previously studied *planar* perylene dimer that was mostly folded in chlorinated solvents,  $K_{\text{fold}}$  in the *twisted* perylene dimer was much smaller in similar solvents because the highly twisted  $\pi$ -system tuned down the  $\pi$ -stacking force. Increasing solvent polarity shifted the equilibrium toward the folded states and revealed that the *folded* homochiral dimer and heterochiral dimer have distinct structures. These folded nanostructures were apparent by absorbance and NMR spectroscopy, while it was determined that intramolecular folding dominated over intermolecular assembly.

The cyclic and linear twisted dimers presented here reveal an inherent chiral molecular assembly code, directing self-assembly, folding, and chemical reactions. The implications are important and will undoubtedly expand the field of self-assembly-directed chemistry. We envision that reactions utilizing temporary  $\pi$ - $\pi$  stacking bonds will become commonplace in supramolecular synthesis.

**Acknowledgment.** The authors acknowledge the support of National Institute of General Medicine Sciences (Grant GM065306). A.D.Q.L. was a Beckman Young Investigation (BYI).

**Supporting Information Available:** Synthesis and characterization of the cyclic and linear dimers and their intermediates. This material is available free of charge via the Internet at <http://pubs.acs.org>.

JA7111959